Journal of Organometallic Chemistry 892 (2019) 75–82

Contents lists available at ScienceDirect

Journal of Organometallic Chemistry

journal homepage: www.elsevier.com/locate/jorganchem

Synthesis, optical spectroscopy, structural, and DFT studies on dimeric iodo-bridged Copper(I) complexes

Ashanul Haque [a, b, **], Rayya A. Al Balushi [c], Idris Juma Al-Busaidi [b], Rashid Ilmi [b], Nawal Al Rasbi [b], Maharaja Jayapal [b], Muhammad S. Khan [b, *], Paul R. Raithby [d, ***]

[a] Department of Chemistry, College of Science, University of Hail, Ha'il, 81451, Saudi Arabia
[b] Department of Chemistry, Sultan Qaboos University, P.O. Box 36, Al-Khod, 123, Oman
[c] Department of Basic Sciences, College of Applied and Health Sciences, A'Sharqiyah University, P.O. Box 42, Ibra, 400, Oman
[d] Department of Chemistry, University of Bath, Claverton Down, Bath, BA2 7AY, UK

ARTICLE INFO

Article history:
Received 23 February 2019
Received in revised form
9 April 2019
Accepted 18 April 2019
Available online 27 April 2019

Keywords:
Copper(I) complexes
Ethynylpyridine
DFT studies
Self-assembly
X-ray crystal structures

ABSTRACT

Three new iodo-bridged copper(I) complexes of the type $[CuI(PPh_3)L]_2$, where L = Ar−≡−C_5H_4N, Ar = phenyl (**C_1**), biphenyl (**C_2**) and flourenyl (**C_3**) have been synthesized *via* coordination-driven self-assembly processes. Two of Cu(I) complexes, **C_2** and **C_3**, have been characterized by single-crystal X-ray diffraction studies. The complexes have two molecules of the P-donor ligand and two molecules of the N-donor ligand in *trans* configurations, supporting the central Cu_2I_2 unit. Absorption properties of the complexes have been investigated. Extensive DFT calculation has been carried out to delineate the influence of aromatic spacers on the optical properties and the nature of excited states. The ease of synthesis of these Cu(I) dimers and the wide range of ethynylpyridine supporting ligands that can be incorporated highlights the potential for these materials to form polymers by linking through the ethylylpyridine ligands.

1. Introduction

Transition metal complexes have attracted significant attention due to their diverse photophysical properties and applications [1–5]. The last four decades has witnessed a great upsurge in the design and development of d^{10} ion-based complexes such as those of copper(I) bearing homo- and heteroleptic ligands [6,7]. Among luminescent transition metal complexes, copper(I)-based systems offer easy synthetic routes, a diverse range of structural arrangements, bright luminescence encompassing a broad range of the visible and UV spectrum, high quantum yields, etc. It has been demonstrated that neutral copper(I) complexes bearing N- and P-coordinating ligands surrounding a halogenido-bridged Cu_2X_2 (X = halogen) core are good candidates for optoelectronic applications [8]. By simple variation of the coordination sphere (i.e. the coordinating and bridging ligands) around the metal, both absorption and emission can be manipulated. For instance, it has been demonstrated that metal to ligand charge transfer (MLCT) or halide to ligand charge transfer (XLCT) emission bands can be significantly tuned by varying the π^* level of ligands [8]. Because of these features, several new copper(I) complexes have been synthesized and tested as components for photovoltaics (PVs), organic-light emitting diodes (OLEDs), sensors, etc. [7,9] The low toxicity and the pseudo-tetrahedral geometry of the complexes has also prompted researchers to assess their biological activity [3].

Within the class of Cu_2X_2 complexes, synthetic manipulation can readily be achieved by altering the nature of the supporting ligands, usually with donor N- or P-bridgehead atoms [10–12]. The pyridine nitrogen donor atom has a strong tendency to interact with a variety of metals and, as a result, a number of complexes bearing simple to functionalized pyridine (or higher pyridines) have been reported [3]. Not only does the electron-deficient pyridine endow structural rigidity, but a judicious choice of functionalization and macrocyclization through pyridine core can also impart helicity/chirality to the resulting complexes [13]. Bearing these features in mind, we have investigated structural and photophysical behavior of a number of acetylide-functionalized

* Corresponding author.
** Corresponding author. Department of Chemistry, College of Science, University of Hail, Ha'il, 81451, Saudi Arabia.
*** Corresponding author.
E-mail addresses: a.haque@uoh.edu.sa (A. Haque), msk@squ.edu.om (M.S. Khan), p.r.raithby@bath.ac.uk (P.R. Raithby).

https://doi.org/10.1016/j.jorganchem.2019.04.017
0022-328X/

pyridinyl copper(I) complexes. Both dimeric and tetrameric copper(I) complexes bearing ethynylpyridinyl-based coordinating ligands have been investigated [5,14,15]. For example, we demonstrated that copper(I) complexes bearing pyridine ligands connected to 4-ethynyl ferrocene show intriguing electrochemical properties. In such complexes, the ferrocene units act as an electron reservoir/sink and was detrimental to the emission properties [15]. Similarly, we recently demonstrated that dye sensitized solar cells (DSSC) based on Cu_2X_2 bridged complexes with heteroarylethynyl attached to 4-position of pyridine (Chart 1) are highly emissive and show up to 2% light to energy conversion efficiency [5]. The performance of the dye was found to depend significantly on two factors: (i) nature of the aryl group attached to pyridine *via* π-linker; and (ii) presence/absence of an anchoring group associated with the phosphine ligands.

To examine the effect of replacing heterocyclic spacers by carbocyclic spacers (such as phenyl, biphenyl and fluorene), we now report the synthesis, structures, photophysical and DFT studies on three new iodo-bridged copper(I) complexes supported by ethylylpyridine-based ligands. The complexes were prepared *via* self-assembly in the solution phase under mild conditions.

2. Experimental

2.1. General

All chemicals and reagents, except where stated otherwise, were obtained commercially and used without further purification. Unless otherwise stated, syntheses were performed under a dry argon atmosphere. Solvents were pre-dried and distilled before use by standard procedures [16]. NMR spectra were recorded on a Bruker AM-400 spectrometer in $CDCl_3$. ^1H NMR spectra were referenced to solvent resonances and $^{31}P\{1H\}$ NMR spectra were referenced to external phosphoric acid. IR spectra were recorded directly on the sample as attenuated total reflectance (ATR) on Diamond using Cary 630 FT-IR spectrometer. UV–vis spectra were recorded with an Agilent Cary 5000 UV–visible spectrophotometer using a quartz cuvette with a 1 cm path length. Column chromatography was performed on either Kieselgel 60 (230–400 mesh) or celite.

2.2. General protocol for the synthesis

2.2.1. Synthesis of ligands (L_1-L_3) and complexes (C_1-C_3)

The intermediates and final products were obtained *via* established cross-coupling reactions [5,15,17]. Briefly, 4-trimethylsililyethynylpyridine was obtained by reacting an equimolar quantity of 4-iodopyridine (2.0 mmol) with trimethylsilylethyne (TMSE, 2.0 mmol) in THF/^{i}PrNH$_2$ using Pd(II)/Cu(I) catalysts (Scheme 1). The crude product obtained was purified by silica column chromatography using hexane/dichloromethane eluant systems. This was followed by a protodesilylation reaction under basic condition (aq. KOH in MeOH/THF) and the 4-ethynylpyridine was separated by silica column chromatography using pure dichloromethane as eluant. In the next phase of the reaction, respective aryl halides (2.0 mmol) and 4-ethynylpyridine (2.0 mmol) were coupled *via* a Sonogashira cross-coupling reaction. Final products were purified using an alumina column and obtained as tan to light brown solid in quantitative yields.

Phenylethynylpyridine (**L_1**): IR (ν_{max}) cm^{-1}: 2199 (-C≡C-), 1598 (C-N), ^1H NMR (700 MHz, $CDCl_3$): δ(ppm) 8.45 (d, 2H, J = 6.4, H-py), 7.98 (d, 2H, *J* = 5.8, H-py), 7.35 (d, 2H, *J* = 6.2, H-Ph), 6.70–6.68 (m, 3H, H-Ph). ESI-MS: *m/z* 179.9 (M+). $C_{13}H_9N$ Anal. Calc.: C, 87.12; H 5.06; N, 7.82%. Found: C, 86.97; H, 4.94; N, 7.77%.

Biphenylethynylpyridine (**L_2**): IR (ν_{max}) cm^{-1}: 2208 (-C≡C-), 1605 (C-N), ^1H NMR (700 MHz, $CDCl_3$): δ(ppm) 8.28 (d, 2H, *J* = 5.95 Hz, H-py), 7.68 (d, 2H, *J* = 4.55 Hz, H-py), 7.62–7.60 (m, 2H, H-biph), 7.46 (dd, 4H, *J* = 5.53, 13.51 Hz, H-biph), 7.38–7.35 (m, 3H,H-biph). ESI-MS: *m/z* 256.1 (M+). $C_{19}H_{13}N$ Anal. Calc.: C, 89.38; H, 5.13; N, 5.49%. Found: C, 8.98; H, 4.83; N, 5.02%.

Fluorenylethynylpyridine (**L_3**): IR (ν_{max}) cm^{-1}: 2205 (-C≡C-), 1608 (C-N), ^1H NMR (700 MHz, $CDCl_3$): δ(ppm) 8.61 (d, 2H, J = 5.74 Hz, H-py), 8.27 (d, 2H, J = 5.95 Hz, H-py), 7.81–7.79 (m, 2H, H-fluorene), 7.78 (s, 1H, H-fluorene), 7.73 (m, 2H, H-fluorene), 7.59–7.57 (m, 2H, H-fluorene), 3.93 (s, 2H). ESI-MS: *m/z* 268.1 (M+). $C_{20}H_{13}N$ Anal.

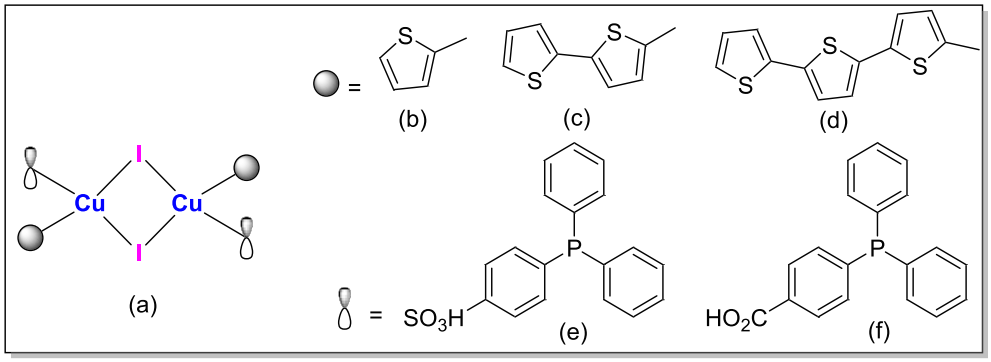

Chart 1. Recently reported acetylide-functionalized pyridine-based Cu(I) complexes for PV applications.

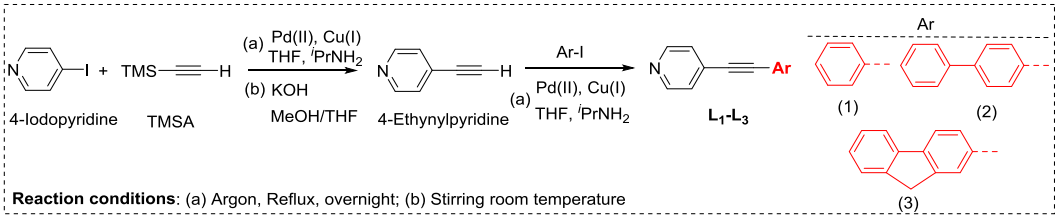

Scheme 1. Synthesis of 4-arylethynylpyridine ligands (**L_1-L_3**).

Calc.: C, 89.86; H, 4.90; N, 5.24%. Found: C, 88.26; H, 4.49; N, 4.94%.

2.2.2. Synthesis of Cu(I) complexes (C_1-C_3)

Cu(I) complexes were synthesized following the protocol reported in literature [5,15,17]. Complexes **C_1-C_3** were obtained by stirring a mixture of the appropriate arylethynylpyridine ligands (1.0 mmol), CuI (1.0 mmol) and triphenylphosphine (1.0 mmol) in an equimolar mixture in degassed dichloromethane (Scheme 2). After stirring for 24 h at room temperature, the mixture was filtered, and the filtrate was concentrated under reduced pressure to produce neutral dimeric complexes **C_1-C_3**. All complexes are stable to light and air and were fully characterized. Crystals suitable for X-ray analysis were obtained by slow diffusion of dichloromethane (DCM) in hexane.

Complex $[L1(CuI)_2(PPh_3)_2]$ (**C_1**): IR: 2206 cm^{-1} ν(C≡C), 1488 cm^{-1} ν(C=N). ^{1}H NMR (700 MHz, $CDCl_3$): δ(ppm) 8.70 (d, J = 5.98 Hz, 4H, H-py), 7.91 (d, J = 6.3 Hz, 8 H, H-py and PPh_3), 7.71–7.42 (m, 36 H, H-Ph and PPh_3). ^{31}PNMR (121.53 MHz, $CDCl_3$): δ = 29.18 (s, PPh_3) ppm. ESI-MS: m/z 1261.9 (M+). $C_{62}H_{48}Cu_2I_2N_2P_2$ Anal. Calc.: C, 58.92; H, 3.83; N, 2.22%. Found: C, 59.55; H, 4.01; N, 2.17%

Complex $[L2(CuI)_2(PPh_3)_2]$ (**C_2**): IR: 2210 cm^{-1} ν(C≡C), 1489 cm^{-1} ν(C=N). ^{1}H NMR (700 MHz, $CDCl_3$): δ(ppm) 8.65 (d, J = 4.48 Hz, 4 H, H-py), 7.62 (d, J = 10.5 Hz, 12 H, H-py and PPh_3), 7.55–7.34 (m, 40 H, H-biph and PPh_3). ^{31}PNMR (121.53 MHz, $CDCl_3$): δ = 29.22 (s, PPh_3) ppm. ESI-MS: m/z 1413.7 (M+). $C_{74}H_{56}Cu_2I_2N_2P_2$: Anal. Calc.: C, 62.76; H, 3.99; N, 1.98%. Found: C, 64.88; H, 4.11; N, 2.01%.

Complex $[L3(CuI)_2(PPh_3)_2]$ (**C_3**): IR: 2208 cm^{-1} ν(C≡C), 1493 cm^{-1} ν(C=N). ^{1}H NMR (700 MHz, $CDCl_3$): δ(ppm) 8.64 (m, 4 H, H-py), 7.81–7.79 (m, 4 H, H-py), 7.74–7.57 (m, 30 H, H-flourene and PPh_3), 7.52–7.34 (m, 14 H, H-flourene and PPh_3), 3.94 (s, 2H). ^{31}PNMR (121.53 MHz, $CDCl_3$): δ = 29.31 (s, PPh_3) ppm. ESI-MS: m/z 1440.2 (M+). $C_{76}H_{56}Cu_2I_2N_2P_2$ Anal. Calc.: C, 63.38; H, 3.92; N, 1.95%. Found: C, 64.88; H, 4.19; N, 2.01%.

2.3. X-ray crystal structure determination

Single-crystal X-ray diffraction experiments were performed at 150(2) K on an Oxford Diffraction Gemini A Ultra CCD diffractometer monochromatic Mo-Kα radiation (λ = 0.71073 Å). The sample temperature was controlled using an Oxford Diffraction Cryojet apparatus; CrysAlis Pro was used for the collection of frames of data, indexing reflections and determining lattice parameters [18]. Structures were solved by direct methods using SIR-92 [19] and refined by full-matric least-squares, on F^2, using SHELXL2014 [20] within the OLEX2 suite of programs [21]. A multi-scan absorption correction was applied in all cases. The hydrogen atoms were generated geometrically and refined with common isotropic thermal parameters. Crystallographic data for the complexes is presented in Table 1. In the case of **C_3**, the fluorene rings showed significant disorder that could not be modelled effectively. As a last resort the unit was assigned isotropic displacement parameters and the carbon atoms were assigned full occupancies. While the refinement was stable with this model several significant residual electron density peaks in the vicinity of the ligand remained. The cif files for the two structures have been deposited with the CCDC: *CCDC 1898577-1898578*.

2.4. Computational studies

2.4.1. Computational details

All DFT calculations were performed using the Gaussian 09 [22] package with the Lee–Yang–Parr correlation function (B3LYP) [23]. For copper and iodide, the Hay and Wadt basis-set LANL2DZ pseudopotential [24,25]. was used. The 6-311 + G(d) [26]. basis-set was employed for N and P, while the 6-31G(d,p) [27] basis-set was

Table 1
Crystallographic data for **C_2-C_3**.

	C_2	C_3
Empirical formula	C_{74} H_{56} Cu_2 I_2 N_2 P_2	C_{76} H_{56} Cu_2 I_2 N_2 P_2
Formula weight	1416.02	1440.04
T(K)	150(2)	150(2)
λ (Å)	0.71073	0.71073
Crystal system	Monoclinic	Monoclinic
Space group	$P2_1/n$	$P2_1/n$
a	9.43370(10)	9.3125(2)
b	22.5428(3)	22.1452(4)
c	14.2331(2)	15.2590(3)
α	90°.	90
β	98.562(1)	101.061(2)
γ	90	90
V (Å^3)	2993.11(7)	3088.36(11)
Z	2	2
$\rho_{calc.}$ Mg m^{-3}	1.571	1.549
μ (Mo-K_α) (mm^{-1})	1.842	1.787
F(000)	1416	1440
Crystal size (mm)	0.60 × 0.40 x 0.40	0.2 × 0.2 x 0.04
θ range (deg)	2.834 to 31.192	2.971 to 29.689
Reflections collected	79295	40941
Independent reflections [R(int)]	9128 [0.0375]	7906 [0.0385]
Completeness to theta = 25.242°	99.90%	99.80%
Max. and min. transmission	1.00 and 0.730	1.000 and 0.9209
Data/restraints/parameters	9128/0/370	7906/0/302
Goodness-of-fit on F^2	1.133	1.034
Final R_1, wR_2 indices [I > 2σ(I)]	0.0305, 0.0584	0.0719, 0.1870
R indices (all data)	0.0454, 0.0647	0.0927, 0.2013
Largest diff. peak, hole (e.Å^{-3})	1.101, −0.516	3.528, −1.267

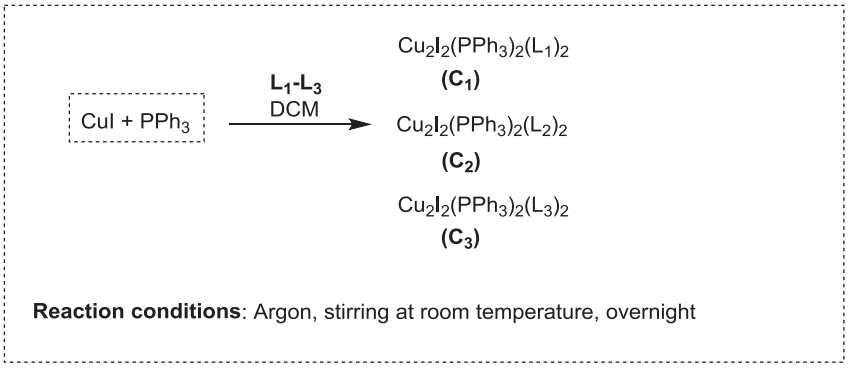

Scheme 2. Synthesis of Cu(I) complexes (**C_1-C_3**).

operated for the atomic orbital of C, H to calculate all the optimized structures. TD-DFT calculations were performed using the same functional and the polarizable continuum model, CPCM with dichloromethane ($\varepsilon = 8.93$) as the surrounding solvent considering bulk solvent effects [28]. TD-DFT-calculated electronic spectra were depicted by using GaussSum, [29] All the molecular orbitals and spin-density diagrams were plotted using the Chemcraft Visualization program [30].

3. Result & discussion

3.1. Synthesis and spectroscopic characterization

The ligands **L_1 L_3** and their corresponding complexes **C_1 C_3** have been synthesized by adapting previously reported procedure [5]. Briefly, arylhalides (4-Iodophenyl, 2-bromobiphenyl or 2-iodofluorenyl) were cross-coupled with TMSA using Sonogashira coupling reaction followed by protodesilylation giving the terminal alkynes (Scheme 1). The deprotected ligands obtained were then coupled with 4-iodopyridine to produce ligands **L_1 L_3** as yellow-brown powders in 60–78% yield. Analytical data (IR, NMR and MS) confirmed the formulation of the ligands. For example, TMSA protection of 4-iodopyridine was confirmed by the observed C≡C-stretching frequency (~2165 cm^{-1}) while deprotection was confirmed by the presence of the C≡H stretching frequency (~3223 cm^{-1}) in addition to the C≡C band. Moreover, the $\nu_{(C\equiv C)}$ value of 4-ethynylpyridine was found to be lower than those of the 4-(trimethylsilylethynyl)pyridine due to the fact that terminal alkynes (HC≡C–R) have lower $\nu_{C\equiv C}$ stretching frequencies than their protected counterparts RC≡CR [31]. The complexes **C_1-C_3** were obtained by swift solution phase self-assembled coordination. The reaction of the ligand (**L_1 L_3**), with copper iodide and triphenyl phosphine (1:1:1 ratio), in dry dichloromethane, under an argon atmosphere produced the complexes **C_1 C_3**. In addition to the standard analytical techniques, single crystal X-ray diffraction studies provided the full three-dimensional molecular and crystal structures of the three complexes.

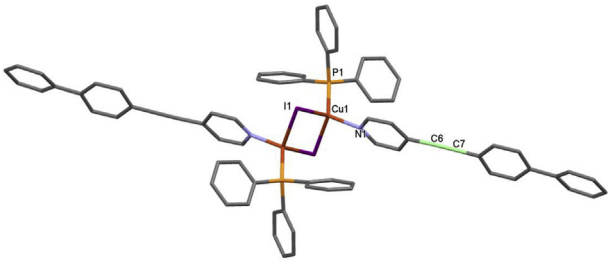

Fig. 1. The crystal structure of the dimeric complex **C_2**. Hydrogen atoms are omitted for clarity.

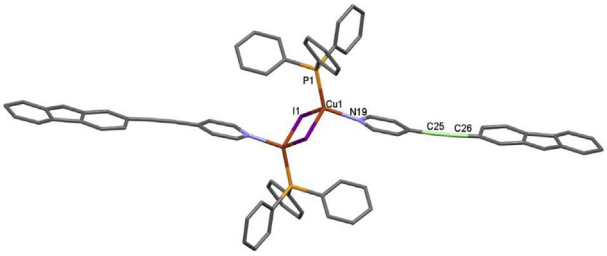

Fig. 2. The crystal structure of the dimeric complex **C_3**. Hydrogen atoms are omitted for clarity.

3.2. Structural characterization

The crystal structures of the complexes: **C_2** and **C_3** were determined and are shown in Figs. 1 and 2. Crystal data is summarized in Table 1 and bond parameters are listed in Tables ST1-ST4 (*supplementary information*). Single crystals of the complexes were obtained by slow diffusion of hexane into a dichloromethane solution of each complex.

The crystal structures of the dimeric complexes **C_2** and **C_3** have a similar planar, parallelepiped Cu_2I_2 core and a *trans* arrangement of the two phosphine and the two **L** ligands. In each case the center of the Cu_2I_2 core sits on a crystallographic center of symmetry, so that the crystallographic asymmetric unit contains half of a dimeric molecule. Each Cu(I) center is in a tetrahedral coordination environment consisting of two bridging iodo ligands, one PPh_3 and the bridgehead nitrogen atom of **L_2** and **L_3**. The unique bond distance for Cu-I, Cu-P and Cu-N are 2.6487(4), 2.2412(6) and 2.063(2) Å, respectively, in **C_2** and are 2.651(8), 2.235(2) and 2.059(6) Å, respectively, in **C_3.** These bond distances are similar to the equivalent bond lengths in a family of previously reported $[(Py)(Ph_3P)CuX]_2$ adducts [32]. The angles at the copper center in the Cu_2I_2 core are obtuse, *e.g.* 111.45(1)° and 108.13(3)° in **C_2** and **C_3,** respectively. While the angle at the iodine center is acute, **e.g.** 68.54(1)° and 71.83(3)° in **C_2** and **C_3,** respectively. The Cu···Cu separations in the dimers: **C_2** (3.0196(5) Å) and **C_3** (3.1394(5) Å), are too long for a formal Cu-Cu bonding interaction; however, it remains similar to reported analogues.

3.3. Optical spectroscopy

The electronic spectra of complexes **C_1-C_3** were measured in

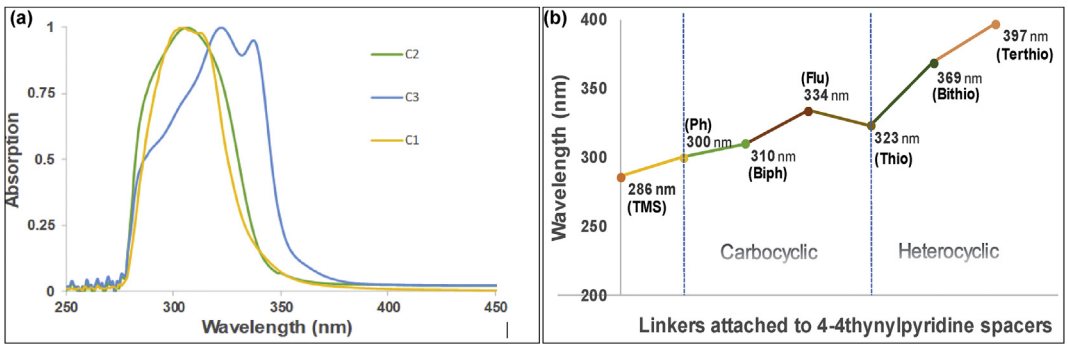

Fig. 3. (a) Normalized UV-vis spectra of complexes **C_1-C_3** in dichloromethane, and (b) the effect of different carbocyclic and heterocyclic aromatic spacers (Ar = Phenyl, biphenyl, fluorene, thiophene, bithiophene and terthiophene) attached to 4-ethynylpyridine ligands in dimeric complexes of type $[L(CuI)_2(PPh_3)_2]$ (where L = Ar–≡–C_6H_4N) on the absorption maxima. Data for the heterocyclic spacers taken from the ref. [5].

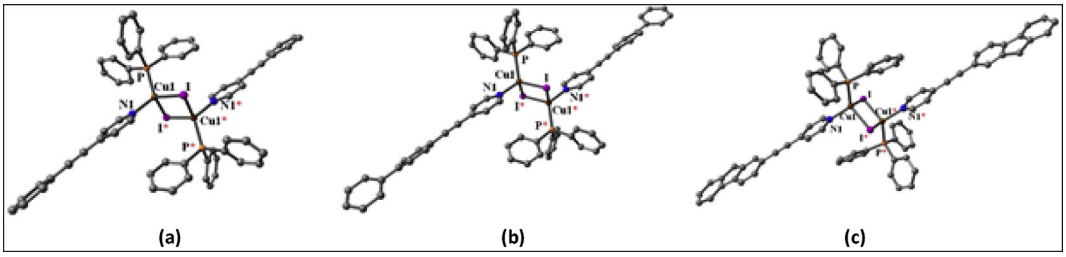

Fig. 4. DFT optimized structures of (a) C_1, (b) C_2, and (c) C_3.

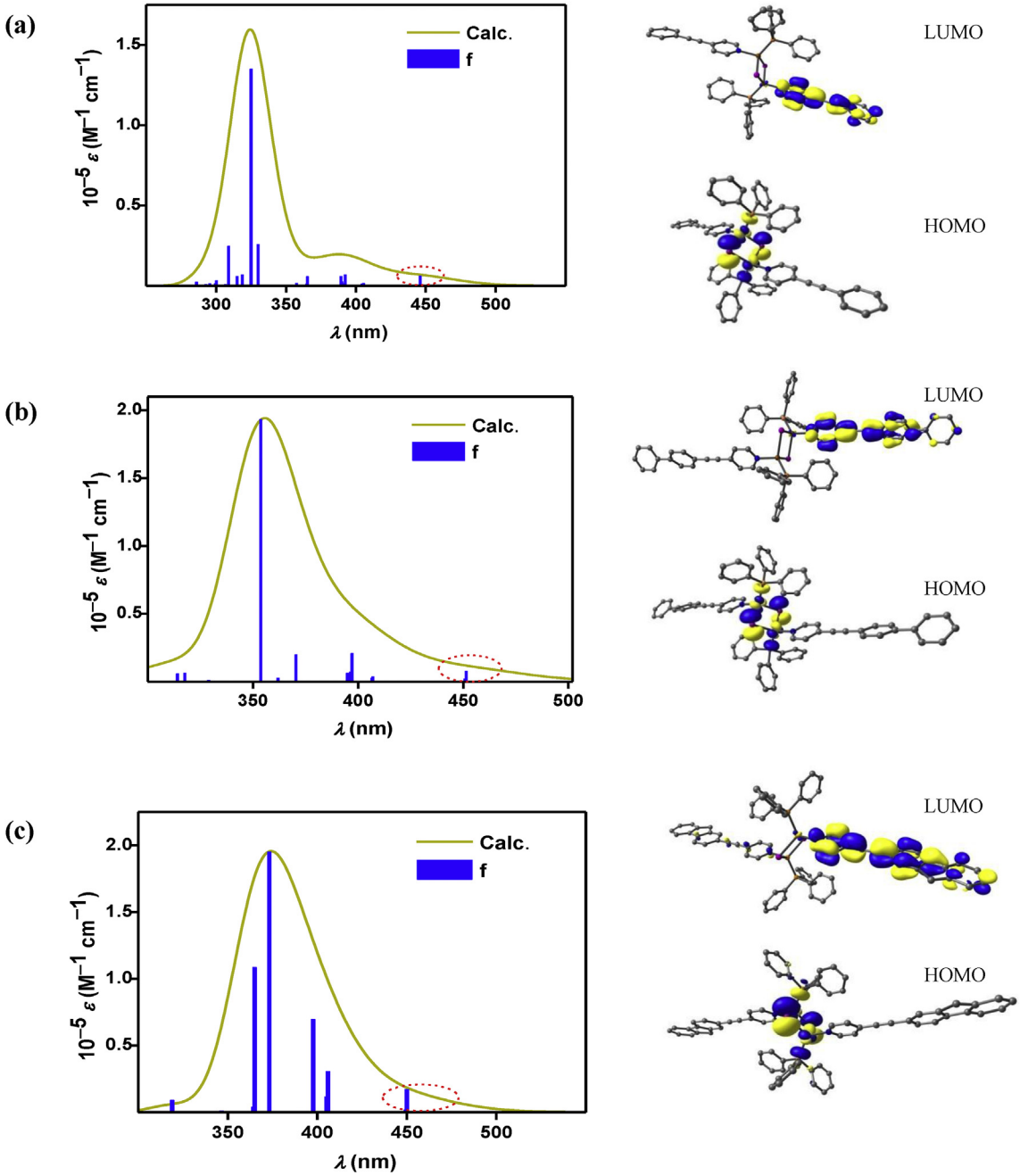

Fig. 5. TD-DFT-Calculated electronic spectra for the Cu(I) complexes (a) C_1, (b) C_2, and (c) C_3 using the B3LYP level of theory. Each plot shows the simulated absorption profile (green), with the bars marked by blue lines representing oscillator strength. Isosurface plots of the highest-occupied and lowest-unoccupied molecular orbitals (HOMOs/LUMOs) for each system are shown to the right of the simulated spectra. (For interpretation of the references to colour in this figure legend, the reader is referred to the Web version of this article.)

DCM at room temperature (Fig. 3a). The onset of absorption for all ethylpyridinyl-based ligands and their corresponding Cu complexes were red-shifted compared to ligand precursor 4-(trimethylsilylethynyl)pyridine ($\lambda_{max} = 286$ nm). The complex incorporating the fluorenylethynylpyridine ligand (**C_3**) showed red-shifted band compared to phenyl and biphenylethnylpyridine Cu(I) complexes (**C_1** and **C_2**). Complex **C_1** showed a strong absorption band at 300 nm (λ_{max}) whereas complexes C_2 and C_3 showed absorptions peaking at 310 and 334 nm, respectively. This can be ascribed to the increasing π-conjugation length leading to a lower energy for the complex and absorption at longer wavelengths. The absorption peaks in the UV spectrum (λ_{max} < 400 nm) can be attributed to the $\pi \rightarrow \pi^*$ transition associated with the arylethynylpyridine group. Fig. 3b shows the effect of attaching different aromatic spacers to 4-ethynylpyridine ligands on the absorption maxima. As expected, the λ_{max} values move to the red (≥10 nm) upon the incorporation of heterocyclic spacers [5]. Comparison of these data with our previous results [5] clearly indicate that the presence of a heavy atom such as sulfur play an important role in shifting the λ_{max} values in dimeric iodo-bridged Cu(I) complexes. As mentioned before, Cu(I) complexes are well known for their emissive properties in both the solid and solution states [8]. In the past, we have demonstrated that the emission properties of ethynylpyridine ligands-based Cu(I) complexes in DCM solution is mainly governed by the electron withdrawing/donating nature of the spacer group. Moreover, there is only little impact of the alkynyl unit (especially for mono-ynes) on the emission wavelength [5]. Therefore, a trend similar to absorption is expected on the emission properties. We are currently investigating the solid-state as well as solution luminescence, electrochemical, thermal and photovoltaic properties of carbocyclic and heterocyclic spacer incorporated ethynylpyridine ligands-based Cu(I) complexes. The results will be communicated separately.

4. DFT calculations

The structures of complexes **C_1-C_3**, bearing three different carbocylic groups (with varying conjugation lengths) attached to the ethynylpyridine ligands were confirmed by DFT calculations employing the B3LYP level of theory (see computational details in the experimental section). Geometry-optimization of complexes **C_2** and **C_3** was performed using the X-ray crystallographic coordinates and the complex **C_1** model was optimized using the same hybrid level of theory. The minima were verified *via* computed vibration frequencies. The DFT calculated bond-lengths and bond-angles of the optimized structures are (Fig. 4 and Table ST5, *supplementary file*) in good agreement with those obtained experimentally (Table ST1-4, *supplementary file*). The time-dependent DFT (TD-DFT) calculations were executed on these optimized geometries to analyze the photophysical properties (Fig. 5). Other frontier molecular orbitals involved in electronic transitions in complexes **C_1-C_3**, as obtained by TD-DFT calculation are shown in Figure SF1-SF3 (*supplementary information*).

To obtain deeper insight of the electronic transitions for all three complexes, TD-DFT calculations have been performed. Here we semi-quantitatively explain the effect of extended conjugation embedded within alkynyl group attached to the pyridyl ligands. The calculated and experimental UV-vis spectra are depicted in Fig. 6. To analyze the spectroscopic activity of these complexes, we have mainly considered the transition in each case with maximum oscillator strengths, *f*, among all the transitions with excitation wavelengths in the 300-400 nm region. From TD-DFT assignments it was revealed that all transitions in this region are largely due to charge-transfer (CT) mainly from the iodide ligands towards the pyridyl rings within the terminally conjugated alkynyl groups. Along with this, there is a substantial contribution of MLCT involving the metal → substituted pyridyl rings. Table 2 and ST6-ST7 (*supplementary information*) lists all excitation energies, wavelengths, oscillator strengths, and an assignment of each state in terms of contributions from individual orbital transitions.

The calculated HOMO−LUMO gaps associated with low energy transitions (~440-450 nm) are also given in the Table 3 though they are not clearly visible experimentally due to the broadening of absorption bands. In complex **C_1**, the brightest transition at nearly 300 nm (experimentally) could be assigned as HOMO−5 to LUMO+1, HOMO−7 to LUMO, and HOMO−8 to LUMO+1 excitations, respectively, with oscillator strengths, $f = 1.62$. We also found a considerably weaker transition between the HOMO and LUMO orbitals at 445 nm ($f = 0.074$). A gradual red shift (Table 3) in the absorption edge (with maximum *f*) of complex **C_2** (310 nm) and complex **C_3** (334 nm) has been observed experimentally, as we move forward from complex **C_1** towards complex **C_3.** This can be explained on the basis of their structural configurations. Due to the incorporation of the more delocalized functionalities into the alkynyl group attached to the pyridyl ligands in Cu(I) complexes, in going from **C_1** to **C_3** a noticeable bathochromic shift is observed in the spectra. Here, the computational modeling also semi-qualitatively represents the key inferences extracted from the optical spectroscopy. It summarized the importance of extended delocalization of the ligands on the frontier orbitals of complex **C_1**

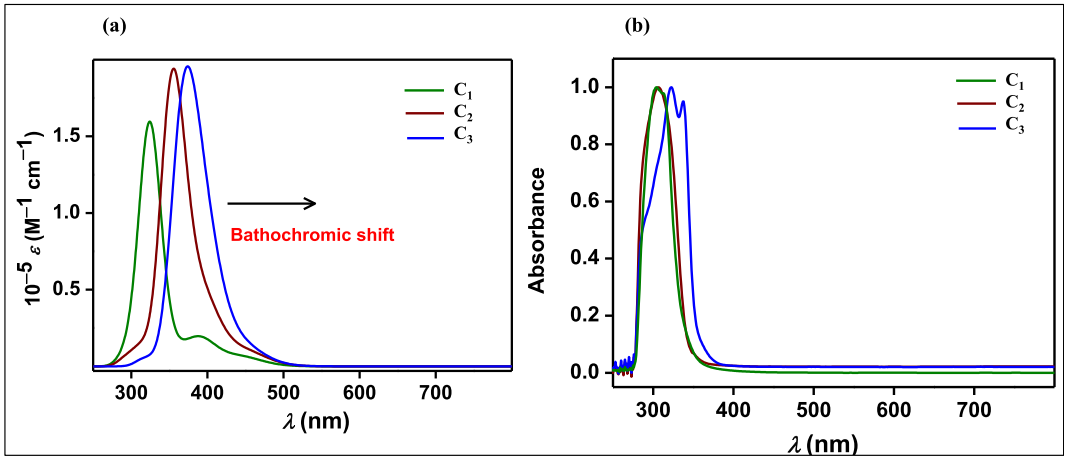

Fig. 6. TD-DFT simulated (**a**) and absorption (**b**) electronic spectra of complexes **C_1-C_3** in DCM.

Table 2
TD-DFT calculated electronic transitions of $\mathbf{C_1}$ using B3LYP level of theory.

Excitation energy (eV)	λ (nm)	*f*	Transition	Character
2.780	445	0.074	α/β-H[~58%L]→ α/β-L [~80%L](92%)	Charge transfer (CT) mainly from iodide towards the pyridyl rings within the terminally conjugated alkynyl groups. A significant contribution of MLCT is also observed involving metal → substituted pyridyl rings.
3.756	330	0.310	α/β-H-3[~57%M]→ α/β-L+1[~89%L](86%)	Combination of MLCT involving metal → substituted pyridyl rings with subsequent CT from iodide towards pyridyl rings within the terminally conjugated alkynyl groups
			α/β-H-5[~63%L]→ α/β-L+1[~89%L](36%)	Charge transfer (CT) mainly from iodide towards the pyridyl rings within the terminally conjugated alkynyl groups. An appreciable contribution of MLCT is also observed here involving metal → substituted pyridyl rings.
3.8144	325	1.62	α/β-H-8[~50%L]→ α/β-L+1[~89%L](28%)	Combination of MLCT involving metal → substituted pyridyl rings with subsequent CT from iodide towards the pyridyl rings within three terminally conjugated alkynyl groups.
			α/β-H-7[~53%M]→ α/β-L [~80%L](66%)	MLCT involving Metal → substituted pyridyl rings with terminally conjugated alkynyl groups and CT in substituted pyridyl rings with terminally conjugated alkynyl groups.
4.013	308	0.295	α/β-H-10[~77%M]→ α/β-L[~80%L](34%)	MLCT involving metal → substituted pyridyl rings within the terminally conjugated alkynyl groups.
			α/β-H-8[~50%L]→ α -L+1[~890%L](46%)	Combination of MLCT involving metal → substituted pyridyl rings with subsequent CT from iodide towards the pyridyl rings within the terminally conjugated alkynyl groups.

Table 3
The calculated HOMO-LUMO gaps associated with low energy transitions, the experimental and calculated λ values.

Complex	Δ(HOMO − LUMO)/kcal/mol	λ (nm)	
		Expt.	DFT calculated
$\mathbf{C_1}$	64.7838	300	324
$\mathbf{C_2}$	74.0262	310	353
$\mathbf{C_3}$	74.1203	334	375

and its analogues leading to red shift across the metal centers and between the aromatic ligands.

5. Conclusion

We have synthesized a range of $[CuI(PPh_3)L]_2$ dimeric complexes, with a Cu_2I_2 core, where L is a series of ethynyl-functionalized pyridine ligands (Ar-C≡C-C_5H_4N), to include the aryl groups phenyl ($\mathbf{C_1}$), biphenyl ($\mathbf{C_2}$) and fluorenyl ($\mathbf{C_3}$) using established coordination-driven self-assembly synthetic strategies. Crystallographic studies confirm the expected *trans* arrangement of the L ligands across the planar parallelepiped Cu_2I_2 core. The UV/visible absorption spectra of the three ethylpyridinyl-based ligands and their corresponding Cu complexes were red-shifted compared to ligand precursor 4-(trimethylsilyl ethynyl)pyridine. In the complexes the magnitude of the red shift increases in the order $\mathbf{C_1} < \mathbf{C_2} < \mathbf{C_3}$ which can be ascribed to the increasing π-conjugation length of the arylethynylpyridine ligand. DFT calculations confirm that the bands in the absorption spectra are a mixture of charge transfer from the iodine ligands to the functionalized pyridine groups and MLCT from the copper centers also to the functionalized pyridine ligands.

This study, coupled with our previous work, [5] indicates that these dinuclear copper (I) systems are amenable to coordination with a wide range of functionalized Ar-C≡C-C_5H_4N ligands, and opens up the possibility of synthesizing one-dimensional polymeric systems *via* further manipulation of the Ar groups to form functionalized linkers through covalent bond formation.

Acknowledgements

AH acknowledges the Department of Chemistry, University of Hail, Kingdom of Saudi Arabia for providing infrastructure support during the preparation of this manuscript. MSK thanks His Majesty's Trust Fund for Strategic Research (Grant No. SR/SQU/SCI/CHEM/16/02) for funding. PRR is grateful to the Engineering and Physical Sciences Research Council (UK) for continued support (EP/K004956/1).

Appendix A. Supplementary data

Supplementary data to this article can be found online at https://doi.org/10.1016/j.jorganchem.2019.04.017.

References

[1] I. Ali, W.A. Wani, A. Khan, A. Haque, A. Ahmad, K. Saleem, N. Manzoor, Synthesis and synergistic antifungal activities of a pyrazoline based ligand and its copper (II) and nickel (II) complexes with conventional antifungals, Microb. Pathog. 53 (2) (2012) 66–73.
[2] K. Saleem, W.A. Wani, A. Haque, M.N. Lone, M.F. Hsieh, M.A. Jairajpuri, I. Ali, Synthesis, DNA binding, hemolysis assays and anticancer studies of copper(II), nickel(II) and iron(III) complexes of a pyrazoline-based ligand, Future Med. Chem. 5 (2) (2013) 135–146.
[3] A. Haque, R. Ilmi, I.J. Al-Busaidi, M.S. Khan, Coordination chemistry and application of mono- and oligopyridine-based macrocycles, Coord. Chem. Rev. 350 (2017) 320–339.
[4] A. Haque, R.A. Al-Balushi, I.J. Al-Busaidi, M.S. Khan, P.R. Raithby, Rise of conjugated poly-ynes and poly(metalla-ynes): from design through synthesis to structure-property relationships and applications, Chem. Rev. 118 (18) (2018) 8474–8597 (and references therein).
[5] M. Jayapal, A. Haque, I.J. Al-Busaidi, N. Al-Rasbi, M.K. Al-Suti, M.S. Khan, R. Al-Balushi, S.M. Islam, C. Xin, W. Wu, W.Y. Wong, F. Marken, P.R. Raithby, Dicopper(I) complexes incorporating acetylide-functionalized pyridinyl-based ligands: synthesis, structural, and photovoltaic studies, Inorg. Chem. 57 (19) (2018) 12113–12124.
[6] R. Peng, M. Li, D. Li, Copper(I) halides: a versatile family in coordination chemistry and crystal engineering, Coord. Chem. Rev. 254 (1) (2010) 1–18.
[7] R. Ilmi, I. Juma Al-busaidi, A. Haque, M.S. Khan, Recent progress in coordination chemistry, photo-physical properties, and applications of pyridine-based Cu (I) complexes, J. Coord. Chem. 71 (19) (2018) 3045–3076.
[8] K. Tsuge, Y. Chishina, H. Hashiguchi, Y. Sasaki, M. Kato, S. Ishizaka, N. Kitamura, Luminescent copper (I) complexes with halogenido-bridged dimeric core, Coord. Chem. Rev. 306 (2016) 636–651.
[9] Y. Liu, S.-C. Yiu, C.-L. Ho, W.-Y. Wong, Recent advances in copper complexes for electrical/light energy conversion, Coord. Chem. Rev. 375 (2018) 514–557.
[10] L. Qi, Q. Li, X. Hong, L. Liu, X.-X. Zhong, Q. Chen, F.-B. Li, Q. Liu, H.-M. Qin, W.-Y. Wong, Synthesis, characterization and luminescent properties of three-coordinate copper (I) halide complexes containing 2-(diphenylphosphino) biphenyl, J. Coord. Chem. 69 (24) (2016) 3692–3702.
[11] B.-L. Chen, L. Liu, X.-X. Zhong, A.M. Asiri, K.A. Alamry, G.-H. Li, F.-B. Li, N.-Y. Zhu, W.-Y. Wong, H.-M. Qin, Synthesis, characterization and luminescent properties of copper (I) halide complexes containing biphenyl bidentate phosphine ligand, J. Coord. Chem. 70 (23) (2017) 3907–3919.
[12] X. Hong, B. Wang, L. Liu, X.-X. Zhong, F.-B. Li, L. Wang, W.-Y. Wong, H.-M. Qin, Y.H. Lo, Highly efficient blue–green neutral dinuclear copper (I) halide complexes containing bidentate phosphine ligands, J. Lumin. 180 (2016) 64–72.
[13] K.F. Sultana, S.Y. Lee, J.-E. Lee, J. Seo, S.S. Lee, Mono-and dinuclear silver (I) complexes of benzene-and pyridine-bearing 20-membered thiaoxaaza macrocycles, Inorg. Chem. Commun. 10 (12) (2007) 1496–1500.
[14] H.H. Shah, R.A. Al-Balushi, M.K. Al-Suti, M.S. Khan, C.H. Woodall, A.L. Sudlow, P.R. Raithby, G. Kociok-Kohn, K.C. Molloy, F. Marken, New multi-ferrocenyl- and multi-ferricenyl- materials via coordination-driven self-assembly and via charge-driven electro-crystallization, Inorg. Chem. 52 (20) (2013)

12012–12022.
[15] H.H. Shah, R.A. Al-Balushi, M.K. Al-Suti, M.S. Khan, F. Marken, A.L. Sudlow, G. Kociok-Kohn, C.H. Woodall, P.R. Raithby, K.C. Molloy, New di-ferrocenyl-ethynylpyridinyl triphenylphosphine copper halide complexes and related di-ferricenyl electro-crystallized materials, Dalton Trans. 43 (25) (2014) 9497–9507.
[16] D.B.G. Williams, M. Lawton, Drying of organic solvents: quantitative evaluation of the efficiency of several desiccants, J. Org. Chem. 75 (24) (2010) 8351–8354.
[17] H.H. Shah, R.A. Al-Balushi, M.K. Al-Suti, M.S. Khan, C.H. Woodall, K.C. Molloy, P.R. Raithby, T.P. Robinson, S.E. Dale, F. Marken, Long-range intramolecular electronic communication in bis (ferrocenylethynyl) complexes incorporating conjugated heterocyclic spacers: synthesis, crystallography, and electrochemistry, Inorg. Chem. 52 (9) (2013) 4898–4908.
[18] CrysAlis Software Package, Oxford Diffraction Ltd, Oxford, UK, 2011, 2011.
[19] A. Altomare, G. Cascarano, C. Giacovazzo, A. Guagliardi, M. Burla, G.t. Polidori, M. Camalli, SIRPOW. 92—a program for automatic solution of crystal structures by direct methods optimized for powder data, J. Appl. Crystallogr. 27 (3) (1994) 435–436.
[20] G.M. Sheldrick, Crystal structure refinement with SHELXL, Acta Crystallogr. C: Struct. Chem. 71 (1) (2015) 3–8.
[21] O.V. Dolomanov, L.J. Bourhis, R.J. Gildea, J.A. Howard, H. Puschmann, OLEX2: a complete structure solution, refinement and analysis program, J. Appl. Crystallogr. 42 (2) (2009) 339–341.
[22] M. Frisch, G. Trucks, H. Schlegel, G. Scuseria, M. Robb, J. Cheeseman, G. Scalmani, V. Barone, B. Mennucci, G. Petersson, 09, Revision D. 01, Gaussian, Inc., Wallingford, CT, 2009.
[23] A. Becke, A.D. Becke, J. Chem. Phys. 98 (1993) 1372. J. Chem. Phys. 98 (1993) 1372.
[24] L. Chiang, A. Kochem, O. Jarjayes, T.J. Dunn, H. Vezin, M. Sakaguchi, T. Ogura, M. Orio, Y. Shimazaki, F. Thomas, Radical localization in a series of symmetric NiII complexes with oxidized salen ligands, Chem. Eur J. 18 (44) (2012) 14117–14127.
[25] P.J. Hay, W.R. Wadt, Ab initio effective core potentials for molecular calculations. Potentials for the transition metal atoms Sc to Hg, J. Chem. Phys. 82 (1) (1985) 270–283.
[26] a. Petersson, A. Bennett, T.G. Tensfeldt, M.A. Al-Laham, W.A. Shirley, J. Mantzaris, A complete basis set model chemistry. I. The total energies of closed-shell atoms and hydrides of the first-row elements, J. Chem. Phys. 89 (4) (1988) 2193–2218.
[27] G. Petersson, M.A. Al-Laham, A complete basis set model chemistry. II. Open-shell systems and the total energies of the first-row atoms, J. Chem. Phys. 94 (9) (1991) 6081–6090.
[28] S. Miertuš, E. Scrocco, J. Tomasi, Electrostatic interaction of a solute with a continuum. A direct utilizaion of AB initio molecular potentials for the prevision of solvent effects, Chem. Phys. 55 (1) (1981) 117–129.
[29] N.M. O'boyle, A.L. Tenderholt, K.M. Langner, Cclib: a library for package-independent computational chemistry algorithms, J. Comput. Chem. 29 (5) (2008) 839–845.
[30] G. Zhurko, D. Zhurko, Chemcraft - Graphical Software for Visualization of Quantum Chemistry Computations. https://www.chemcraftprog.com.
[31] J. Lambert, H. Shurvell, D. Lightner, R. Cooks, Introduction to Organic SpectroscopyMacmillan, New York, 1987, p. 351.
[32] L. Engelhardt, P. Healy, J. Kildea, A. White, Lewis-base adducts of group 11 metal (I) compounds. XLII.[Cu4X4L4]'Cubane'Clusters, L= hindered N-base ligand: synthesis and structure of the L= 2-(diphenylmethyl) pyridine complexes (X= Cl, Br, I), Aust. J. Chem. 42 (1) (1989) 107–113.